

Article

Design and Implementation of a Multi-Function Hydrophone for Underwater Acoustic Application

Rong Wang^{1,2,*}, Yuehai Zhou^{1,2,*}, Xiaoyu Yang^{1,2}, Feng Tong^{1,2} and Jianming Wu^{1,2}

¹ College of Ocean and Earth Sciences, Xiamen University, Xiamen 361102, China; wangrong@stu.xmu.edu.cn (R.W.); xiaoyuyang@stu.xmu.edu.cn (X.Y.); ftong@xmu.edu.cn (F.T.); wjm@xmu.edu.cn (J.W.)

² The National and Local Joint Engineering Research Center for Navigation and Location Service Technology, Xiamen University, Xiamen 361102, China

* Correspondence: zhouyuehai@xmu.edu.cn

Abstract: In recent years, underwater acoustic applications have attracted much attention, for example, for underwater environmental monitoring, underwater exploration, etc. Hydrophones play a particularly important role. Although hydrophone design has been in multifarious application forms, it still needs to consider increasing demand for low-cost, low-consumption, and multiple-function devices, as well as issues around miniaturization, lossless data collection, etc. In this paper, we design a compact underwater acoustic device that has the capability of underwater acoustic signal storage, underwater acoustic signal transmission via the Internet, and decoding based on the direct sequences spread spectrum (DSSS). The key problem is how to implement multiple functions in only one micro-controller unit (MCU). The hardware and software of the proposed multi-function hydrophone are described in detail. In particular, the MCU, the pre-amplifier with gain control, and the analog-to-digital integrated chip are introduced. Moreover, underwater acoustic data storage, underwater acoustic transmission, and the DSSS receiver are depicted in terms of software. The different functions of the hydrophone are verified in sea trial experiments. The results show that the proposed multi-function hydrophone is able to sample underwater acoustic data at high quality. In addition, to demonstrate configurable parameters, the DSSS receiver with different carrier frequencies is provided. The proposed multi-function hydrophone realizes zero bit error rate (BER) when carrier frequency $f_c = 9$ kHz, and the BER with 10^{-3} order of magnitude when carrier frequency $f_c = 15.5$ kHz. The results show that the proposed multi-function hydrophone has great potential to explore the ocean.

Keywords: multi-function hydrophone; underwater acoustic data acquisition; real-time transmission; parameter configuration; DSSS receiver



Citation: Wang, R.; Zhou, Y.; Yang, X.; Tong, F.; Wu, J. Design and Implementation of a Multi-Function Hydrophone for Underwater Acoustic Application. *J. Mar. Sci. Eng.* **2023**, *11*, 2203. <https://doi.org/10.3390/jmse11112203>

Academic Editors: Pavel Petrov, Matthias Ehrhardt and Sergey Pereselkov

Received: 20 September 2023

Revised: 10 November 2023

Accepted: 13 November 2023

Published: 20 November 2023



Copyright: © 2023 by the authors. Licensee MDPI, Basel, Switzerland. This article is an open access article distributed under the terms and conditions of the Creative Commons Attribution (CC BY) license (<https://creativecommons.org/licenses/by/4.0/>).

1. Introduction

The electromagnetic signal attenuates significantly in the water, hence it cannot transmit over a long range. On the contrary, the underwater acoustic signal attenuates far less than the electromagnetic signal, and as a result, underwater sounds widely exist in the ocean from the surface to the bottom. For example, the sound of raindrops and tides, the sound of marine animals, and the sound of tsunamis and under-sea earthquakes. In addition, there is plentiful sound produced by human activities, for example, ship noise, signals for underwater acoustic communication, signals for underwater acoustic ranging, etc. As a result, underwater sound monitoring, storage, and processing become more and more important.

More than 70% of the Earth's surface is covered by ocean and most of the ocean remains unexplored. While rapidly exploring the ocean, more and more in situ data are required to be transmitted or saved. However, devices for recording such in situ data

are not widely developed, or the function of such devices is unitary. The design and implementation of smart ocean equipment are urgent and significant issues.

To date, there have been some systems for underwater acoustic applications. Passive acoustic monitoring systems are extremely valuable for long-term research in the marine environment [1]. With increasing concern about underwater acoustics, numerous studies have proposed analyzing ocean sound [2]. Some surface buoys are capable of streaming acoustic data to shore stations in real time for processing [3]. Ref. [4] described a distributed system for real-time environmental monitoring. Other methods used to measure acoustic signals are moving platforms, such as moored autonomous recorders, underwater gliders [5,6], etc. Although the systems mentioned above easily acquire underwater acoustic signals, they have some shortcomings, for example, the size is quite big, the power consumption is high, the function is unitary, and the parameters are not configurable.

Despite the passive acoustic measurements, active underwater acoustic measurement is very important for exploring the ocean. In one paper [7], a real-time underwater ranging system between commodity hydrophones was designed. To address the severe underwater multi-path, a dual-microphone optimization algorithm that identify the direct path more reliably was researched. The proposed system had median errors of 0.48–0.86 m at distances of up to 35 m.

Underwater acoustic communication and networking have been paid more attention since more information from underwater sensors is required to be exchanged remotely. Many hydrophones have been parts of underwater acoustic MODEMs. For example, in [8], low-power and low bit error rate (BER) amplitude shift keying (ASK), acoustic MODEMs were designed by using STM32F103 (STMicroelectronics, Paris, France), the BER was about 10^{-3} at the distance of 100 m, while when the distance was about 500 m, the BER was approximately 10^{-1} . A hydrophone was used to design on-off keying (OOK) acoustic MODEMs for video-capable with a high data rate in excess of 1 Mbps over 100 m in shallow water [9,10]. In one paper [11], an underwater acoustic orthogonal frequency division multiplexing (OFDM) MODEM was designed, the maximum data rate could reach 5200 bps at a distance of 1000 m. Moreover, the number of null sub-carriers, pilot sub-carriers, and receivers in the MODEM in [11] were all configurable. In another paper [12], an underwater acoustic orthogonal signal division multiplexing (OSDM) MODEM was designed. The OSDM communication method is a compromise between single carriers and the OFDM, so the OSDM MODEM was state-of-the-art. Both shallow-water experiments and deep-sea experiments verified the robustness of the proposed OSDM MODEM.

Currently, there is some related literature about recording underwater acoustic data streams. In one work [1], cost-efficient, innovative, and interoperable ocean passive acoustic sensor systems were developed. The first digital hydrophone system was standalone and was used to record the raw underwater acoustic data. The second digital hydrophone system was a digital passive acoustic transducer array whose main capability was to provide directional sound source information for hydroacoustic surveys. In another work [13], the raw underwater acoustic data stream was recorded by an underwater acoustic MODEM, and a secure digital (SD) card with 64 GB capacity was used to store raw signals. Unfortunately, such application costs high power consumption, and the storage is limited. An underwater acoustic recorder was designed using a single board computer [14], the maximum sampling frequency was 48 kilo-symbols per second (kSPS), and the power consumption was about 1.5 watts.

The current design of digital hydrophones has become more mature. From the perspective of new products launched in recent years, many devices were developed by different famous companies. For example, the smart digital hydrophone named iCListen was developed by Ocean Sonics [15]. iCListen can be used as an acoustic recorder, it has ultra-low noise and a wide bandwidth range from 10 Hz to 200 kHz. There are many series of iCListens for different applications, for more details, please refer to the website [15]. A snap recorder for storing the underwater acoustic data stream was developed by Loggerhead Instruments company [16], the maximum sampling frequency was 96 kHz, and the

maximum working depth was 7000 m when a titanium case was used. There are also some other commercial smart hydrophones. For example, the remote underwater digital acoustic recorder was designed by Cetacean Research Technology [17], the SoundTrap recorder was designed by Ocean Instruments [18], and the DORI underwater acoustic recorder was designed by Abyssens [19].

Many different underwater acoustic devices have been designed in recent years. However, such devices typically have a single function, or their parameters are not configurable, or they have high power consumption, do not have a compact size, etc. In addition, the use of commercial underwater recorders is not the best and feasible choice, since their high cost and lack of flexibility. Multi-function and parameters-configurable underwater acoustic device design is a new trend and requirement, since it is suitable for autonomous underwater vehicles (AUVs), unmanned underwater vehicles (UUVs), etc. The key technical difficulty is how to implement such multiple functions under the limited resources of a micro-controller unit (MCU). To address the problems mentioned above, a compact, multi-function, parameters-configurable hydrophone is designed and implemented in this paper. In particular, the multiple functions include local data preservation, real-time raw data upload, and direct sequence spread spectrum (DSSS) receiver. The software and the hardware of the proposed multi-function hydrophone are introduced in detail. Specifically, the principles and the flowcharts of different functions are described. The pre-amplifier, the analog-to-digital converter (ADC), and MCU are also depicted. To address the limited resources of MCU, memory multiplex is used, and some integrated algorithms from the digital signal processing (DSP) library are used to improve efficiency. Finally, sea trials verified the proposed multi-function hydrophone. The trial results demonstrate that the proposed multi-function hydrophone has good potential to explore the ocean. The proposed multi-function hydrophone can be used for underwater acoustic communication, underwater ambient noise collection and analysis, marine pre-warning, etc.

The remaining paper is organized as follows. Section 2 describes the system overview including the hardware and the software. In Section 3, the experimental results are described and analyzed in detail. Finally, some conclusions are drawn in Section 4.

2. System Overview

The prototype of the proposed multi-function hydrophone is shown in Figure 1. The multi-function hydrophone consists of a piezoelectric ceramic hydrophone, a watertight compartment, and a connection. Respectively, the purposes of those components are to transform the acoustic signals to electromagnetic signals, to protect the battery and hardware, and to connect cables. The length of the multi-function hydrophone is 450 mm, and the diameter is 60 mm. The weight in the air is approximately 2.5 kg, and the power consumption in continuous working mode is about 1.8 watts. The duration of continuous working time is 7 days. The maximum capacity of the SD card is 2 TB. The working frequency band is 20 Hz to 200 kHz. The average receiving sensitivity is about -205 dB @ 1 V/ μ Pa. The maximum sampling frequency is 256 kSPS, and the maximum gain of pre-amplifier is 56.1 dB. The parameters of our multi-function hydrophone are summarized in Table 1.



Figure 1. The overview of hardware.

In the following subsections, the details of the multi-function hydrophone are described in terms of hardware and software.

Table 1. Parameters of the multi-function hydrophone.

Parameter	Value	Parameter	Value
Height	450 mm	Diameter	60 mm
Weight	≈2.5 kg in the air	Power consumption	1.8 Watt
Working time	7 days	Capacity of SD card	maximum 2 TB
Bandwidth	20 Hz–200 kHz	Sensitivity	−205 dB @ V/μPa
Maximum sampling frequency	256 kSPS	Maximum gain	56.1 dB
Average self-noise	no more than 0.1 mV		

2.1. Hardware Design

Since the voltage received by hydrophones is ultra-low, the weak signals should be enlarged by a pre-amplifier, and then processed by MCU after ADC as shown in Figure 2. In the following subsections, each component is introduced.

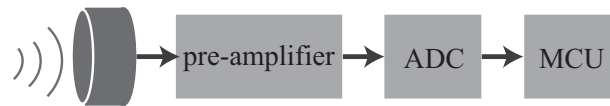


Figure 2. Signal process component.

2.1.1. The Pre-Amplifier

In order to amplify the weak signals, a second-order pre-amplifier is utilized. The integrated chip AD620 is used as the first pre-amplifier. AD620 chip is an instrumentation amplifier [20], and the gain range is from 1 V/V to 10,000 V/V with extremely low noise, where V/V represents the ratio unit of output voltage to input voltage. The gain of AD620 can be adjusted by a resistor R_3 as shown in Figure 3a. The input for AD620 can be single end or differential. The input impedance of AD620 (Analog Devices, Inc., Norwood, MA, USA) is 10 MΩ, which is good for improving the signal to noise ratio (SNR). Moreover, the AD620 chip has some characteristics, e.g., low input offset voltage and input offset drift, high common-mode rejection ratio, etc. A pre-amplifier with an adjustable gain is a good method to counteract the attenuation. Since the MCU contains rich general purpose input output (GPIO), digitally controlled programmable gain amplifier is chosen in our proposed system. As a result, the integrated chip LTC6910-2 ((Analog Devices, Inc., Norwood, MA, USA)) is adopted as a second pre-amplifier as shown in Figure 3b. The gain can be configured as 0 V/V, 1 V/V, 2 V/V, 4 V/V, 8 V/V, 16 V/V, 32 V/V, and 64 V/V, respectively, [21]. Especially, 0 V/V means the input circuit is open while the output is active.

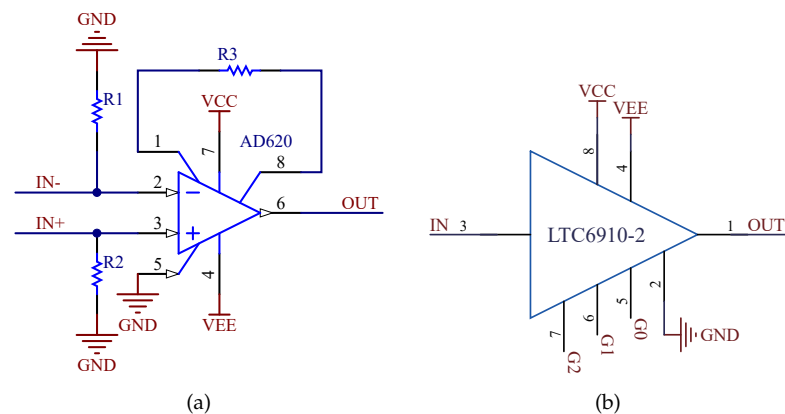


Figure 3. Pre-amplifier. (a) The circuit of AD620. (b) The circuit of LTC6910-2.

2.1.2. The Analog-to-Digital Converter

Considering the sampling rate and the sampling precision, the AD7768-4 chip (Analog Devices, Inc., Norwood, MA, USA) is chosen. Developed by the Analog Device company, the AD7768-4 is widely used in underwater acoustic applications because of its high performance. The AD7768-4 is integrated with four identical and simultaneous channels. The sampling frequency can be configured as 32 kSPS, 64 kSPS, 128 kSPS, and 256 kSPS, respectively. The dynamic range is 108 dB, and the sampling precision is 24 bits, which are able to measure the tiny variations of acoustic signals. The highest power consumption of each channel is 51.5 mW, which is suitable for long-time signal acquisition. In our system, the first channel is used, and the remaining channels are reserved for further use and working in sleep mode. The serial peripheral interface (SPI) is used to set the parameters, and the multichannel audio serial port (MCASP) is used for digital signal transmission.

2.1.3. The Micro-Controller and Peripheral

The MCU is a STM32H743 (STMicroelectronics, Paris, France) which is developed by STMicroelectronics (ST). Integrated with the ARM[®] Cortex[®]-M7 core, the STM32H743 is a compromise between power consumption and computability. When STM32H743 works in standby mode, the current reaches as low as 2.95 μ A. The STM32H743 is integrated with a double-precision floating point unit (FPU) and L1 cache, the frequency is up to 480 MHz, and the computability can reach 2424 CoreMark/1027 dhrystone million instructions per second (DMIPS) [22]. The peripherals are shown in Figure 4. The universal synchronous/asynchronous receiver/transmitter (USART) is used for interacting with the host computer when debugging the program; the Ethernet is used for setting parameters and uploading raw acoustic signals, the purpose of the real-time clock (RTC) is to trace the time, and the function of SD card is used to store the raw acoustic data and log files. In addition, the power management is used to provide different voltages and control the power consumption. Finally, the GPIO is used to control the gain of the pre-amplifier.

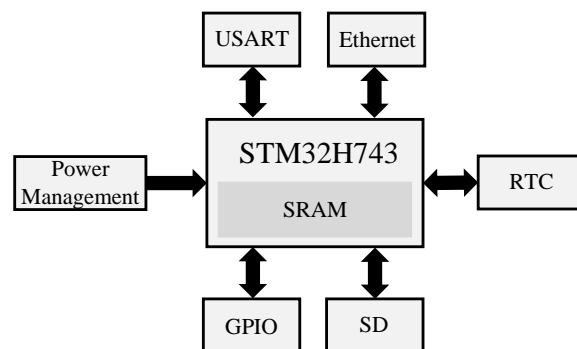


Figure 4. The MCU and its peripherals.

2.2. Software Design

Figure 5 shows the overview of software design, and each rectangle represents a thread. A real-time operating system named FreeRTOS is utilized for the proposed multi-function hydrophone, because it is easy to add different components, such as file system, transmission control protocol/internet protocol (TCP/IP) stack, etc. Moreover, FreeRTOS is a preemptive scheduling system, which is fast to respond to different events. In the proposed multi-function hydrophone design, the Fat32 file system is used. As a result, the computer can read the files directly. In the TCP/IP stack, file transfer protocol (FTP) service, Web service, user datagram protocol (UDP) communication, and TCP communication are easily configured and used. The main thread is used for interaction between threads and users, the controlling data are used for creating or terminating the four sub-threads. Specifically, the “raw data storage” thread, the “raw data transmission” thread, and the

“DSSS demodulation” thread are mutually exclusive, that is to say, only one thread can be executed at one time. In the following, the four sub-threads are introduced.

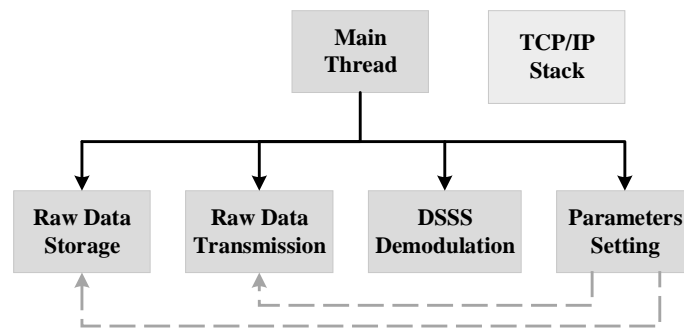


Figure 5. The flowchart of different threads.

2.2.1. Local Data Preservation

The purpose of the “raw data storage” thread is to sample raw acoustic data and save it into the SD card. Unfortunately, the STM32H743 only has one MCU, and the two tasks cannot be performed by one MCU simultaneously. Thanks to the direct memory access (DMA) mechanism which transmits digital data via bus without MCU interaction, the data from AD7768 via MCASP can be fetched to memory, then central processing unit (CPU) writes the data into SD card. Those two processes are performed simultaneously. The data flowchart of “raw data storage” thread is shown in Figure 6. There are two buffers which are named ping buffer and pong buffer, respectively. To avoid data loss when writing data onto the SD card, a ring buffer is used. The purpose of the ring buffer is to manage the writing speed of the SD card. When the ping buffer fetches the acoustic data which is occupied by DMA, the pong buffer is free, so the MCU copies the data to the ring buffer, and the MCU writes the data from the ring buffer to the SD card, and vice versa. The switching between ping buffer and pong buffer is performed by a DMA controller. The raw acoustic data are stored in waveform (WAV) format, and the name of the file is made up of time and date, which can be obtained from the RTC.

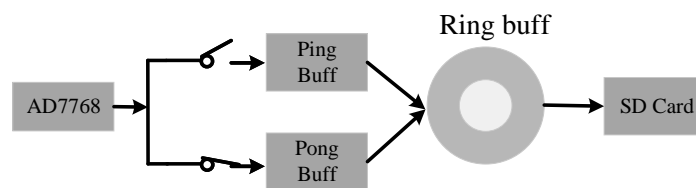


Figure 6. Data flowchart of “raw data storage” thread.

This thread is defined as “mode 1”.

2.2.2. Data Uploading

Since the limitation of MCU for digital signal processing, some emergency data cannot be processed in real time. To address it, such emergency data can be uploaded to a powerful host computer, therefore the results can be measured at once. The diagram of data uploading is shown in Figure 7. When using this function, an additional cable and gateway are required. The gateway can communicate with satellites, or establish local area networks such as WIFI, so researchers in the laboratory or on the ship can receive and analyze the raw acoustic data in time. UDP is a good choice because when it loses connection, it does not require a re-connection, and the transmission will continue. In this mode, the ring buffer is no longer required. When the ping buffer is occupied by DMA, the data from the pong buffer is uploaded to the gateway, and vice versa.

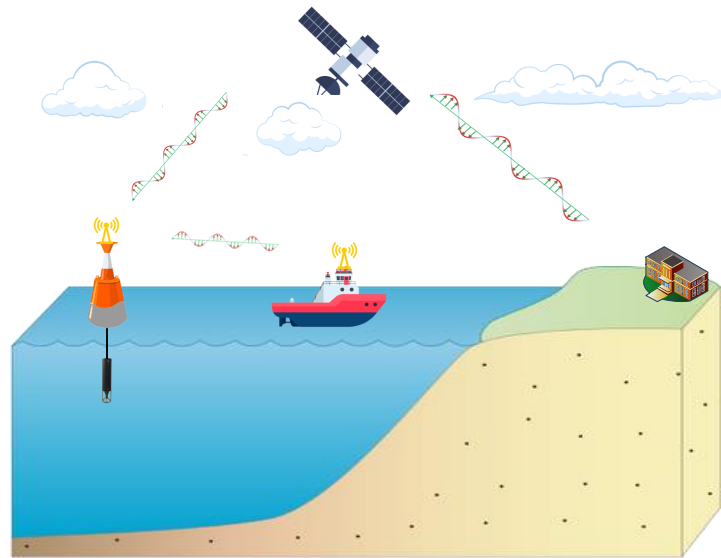


Figure 7. The diagram of data uploading.

This thread is defined as “mode 2”.

2.2.3. Spread Spectrum Communication Technology

The spread spectrum technology has the advantages of anti-noise, anti-interception, and anti-multipath. DSSS can effectively improve the communication range by making full use of the autocorrelation and cross-correlation performance of pseudorandom codes. And because the pseudorandom sequences in use are only known by the transmitter and the receiver, spectrum surveillance is difficult [23]. Thus, DSSS is used in secure communication systems and even in military systems. The DSSS receiver is implemented in the proposed multi-function hydrophone.

Figure 8 shows the diagram of the DSSS receiver. In this mode, the double-buffered mechanism is also used. Please refer to our previous work for how to synchronize the signal frame. After synchronization, the received signal is fetched symbol by symbol, then the digital bandpass filter is adopted to improve SNR, and then carrier demodulation and lowpass filtering are performed symbol by symbol, as shown in (1),

$$\hat{\mathbf{y}} = LPF(\mathbf{r} * \mathbf{c}) , \tag{1}$$

where $LPF(\cdot)$ denotes the lowpass filtering, \mathbf{r} denotes the received DSSS symbol in the passband, \mathbf{c} denotes the local carrier, and $*$ denotes vector multiplication. The downsampling is performed to obtain the baseband signal which is denoted as \mathbf{y} . The next step is the despreading process whose main algorithm is matched filtering. The received baseband signal correlates with multiple local Pseudo noise (PN) sequences, and then find the index of local PN that has the best correlation with the received signals,

$$\lambda = \arg \max(\max(\mathbf{y} \otimes \gamma_i)) . \tag{2}$$

The binary bits are obtained via symbol demapping from λ . Finally, the transmitted bits are recovered after convolutional decoding. For more details about DSSS, please refer to [24].

This thread is defined as “mode 3”.

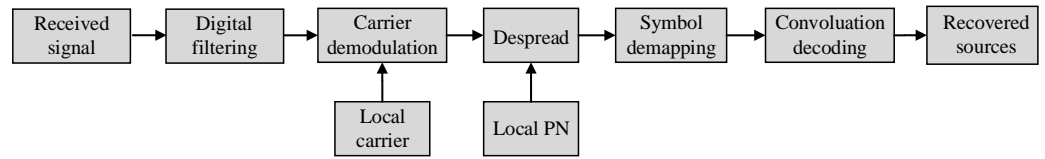


Figure 8. Schematic diagram of M-ary spread spectrum.

2.2.4. Parameters Setting

In our proposed multi-function hydrophone, some parameters are configurable. To ease operation, we designed a graphical user interface (GUI) to control the configurable parameters as shown in Figure 9. The working mode, the sampling frequency, the file length which is written into SD card, and the gain of pre-amplifier can be configured by drop-down lists. Also, the IP and port are configurable which avoids conflicts in the local area network. In addition, the purpose of the “set time” button is to set the RTC with the current time. The two graphs are used to show the signals in the time domain and the frequency domain, respectively, in mode 2.

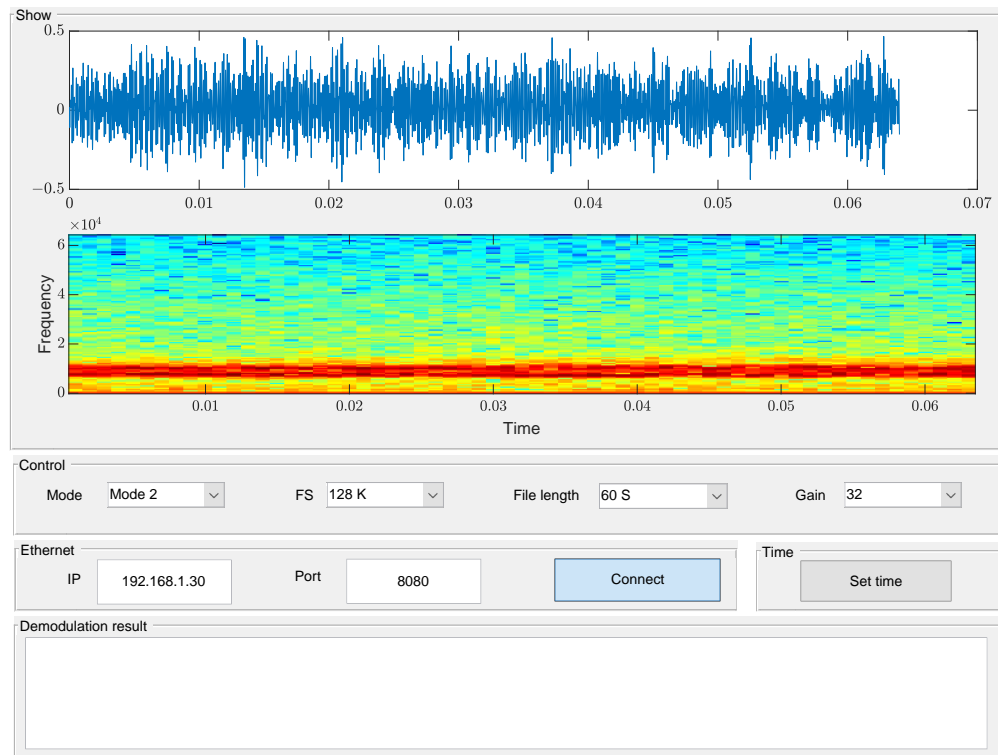


Figure 9. Control interface of the host computer.

3. Results and Analysis

To verify the reliability and stability of the multi-function hydrophone, an experiment was conducted in Wuyuan Bay, Xiamen City, Fujian Province, China. The deployment of the experiment is shown in Figure 10a. The depth of the experimental area was about 10 m. The distance between the transmitter and the proposed hydrophone was about 1 km. And seven multi-function hydrophones were deployed at different depths with a uniform space of 1.2 m. Two transducers with different center frequencies were used to evaluate the performance, the source level of the two transducers is 190 dB @ μPa. The depth of the transmitters was about 5 m. In the experiment, the sea was relatively calm with level 2 sea conditions.

Figure 10b shows the sound speed profile (SSP). Due to the sun exposure, the SSP shows a negative gradient.

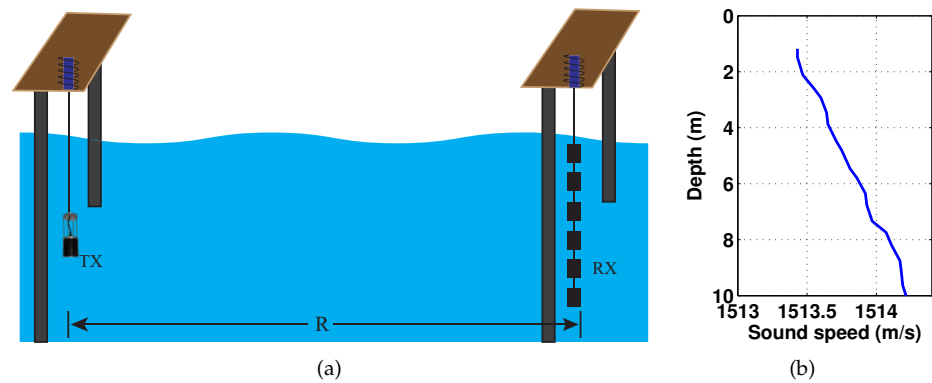


Figure 10. The diagram of deployment and the sound speed profile. (a) The diagram of deployment. (b) The sound speed profile.

The gain of AD620 was fixed at 10 V/V, and the gain of LTC6910-2 was 64 V/V, so the total gain was 56.1 dB (640 V/V). In mode 1, the sampling frequency was 128 kHz, while in mode 2 and mode 3, the sampling frequency was 64 kHz.

3.1. Experimental Results in Mode 1

In mode 1, raw underwater acoustic data are stored on an SD card. The file names consist of the serial number, date, time, and file number. By using such a file name, the users can read and analyze the corresponding signals. Figure 11a shows a signal waveform of the underwater acoustic data saved on the SD card, the signal was linear frequency modulation (LFM). From Figure 11a, one may see that the SNR is very high, which demonstrates the effectiveness of the data reception and preservation. Figure 11b shows the corresponding spectrum, the bandwidth of the LFM signal was 13 kHz to 18 kHz. After the bandpass filter, the average SNR is 19.9 dB.

In a word, the proposed multi-function hydrophone acquires underwater acoustic signals with high resolution and accuracy.

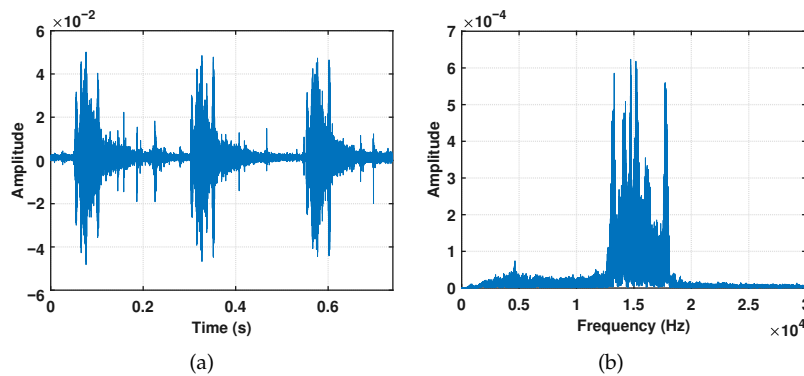


Figure 11. Diagram of the received signal. (a) Time domain diagram. (b) The spectrum diagram.

3.2. Experimental Results in Mode 2

In this subsection, the results of mode 2 are described. The experiment was also conducted in Wuyuan Bay, Xiamen, China. The depths of the hydrophones at 3 m, 6 m, and 9 m were chosen. Three multi-function hydrophones were connected to a router, and the router was connected to a gateway called “Bulltin”. The “Bulltin” transmitted the wired signals to WIFI, and a host computer on the shore received the signals. There are two threads in the host computer, the first thread retrieves raw acoustic signal and saves it into a cache, and the second thread acts as a receiver, which decodes the transmitted symbol online. For single-carrier underwater acoustic communication, the common channel equalization approaches in the time domain are the channel estimation-based decision

feedback equalizer (CE-DFE), and the direct adaptive decision feedback equalizer (DA-DFE). The DA-DFE requires long training sequences to achieve convergence. Compared to DA-DFE, the CE-DFE approach directly measures the channel via shorter training sequences and calculates the channel equalizer’s filters based on channel estimation [25]. It needs less controlling parameters to achieve faster convergence and obtains lower output error. Considering the merit of CE-DFE, a receiver based on CE-DFE was used in the host computer.

The structure of CE-DFE is shown in Figure 12. In Figure 12, notations $y_1, y_2,$ and y_3 are the received signals from three multi-function hydrophones, x_s is the soft output of CE-DFE, and \hat{x} is the hard output of CE-DFE. The soft output of CE-DFE can be written as

$$x_s(i) = \mathbf{f}^H \mathbf{r}, \tag{3}$$

where \mathbf{f} is defined as $\mathbf{f} = (\mathbf{g}_{ff_1}^H, \mathbf{g}_{ff_2}^H, \mathbf{g}_{ff_3}^H, \mathbf{g}_{fb}^H)^H$, \mathbf{r} is defined as $\mathbf{r} = (y_1^H, y_2^H, y_3^H, \hat{x}^H)^H$. Then the optimal filter can be obtained by solving the cost function

$$\hat{\mathbf{f}} = \arg \min_{\mathbf{f}} \|\mathbf{f}^H \mathbf{r} - \mathbf{s}(i)\|_2^2. \tag{4}$$

Finally, the filters can be obtained

$$\mathbf{g}_{ff} = (\mathbf{g}\mathbf{g}^H + \mathbf{D})^{-1} \mathbf{g} \tag{5}$$

$$\mathbf{g}_{fb} = -\mathbf{F}^H (\mathbf{g}\mathbf{g}^H + \mathbf{D})^{-1} \mathbf{g} \tag{6}$$

In (5), \mathbf{g}_{ff} is defined as $\mathbf{g}_{ff} = (\mathbf{g}_{ff_1}^H, \mathbf{g}_{ff_2}^H, \mathbf{g}_{ff_3}^H)^H$. Please refer to [25] for more details about the derivation of (5), (6), \mathbf{F} , and \mathbf{g} .

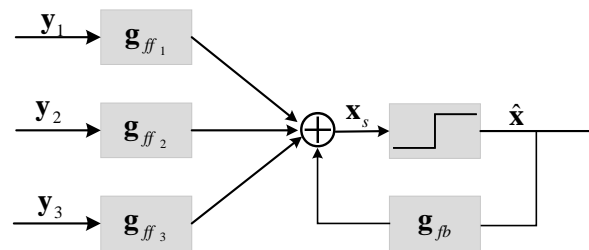


Figure 12. Structure of CE-DFE.

Some parameters in this experiment are shown in Table 2. Based on [26], the longer the length of the feedback filter, the better communication performance it achieves. And the length of the feedback filter should be less than the channel length. Considering the computational complexity and our previous work in [25,27], the length of the feedforward filter is set three times of channel length, and the length of the feedback filter is set approximate to the channel length. The discrete channel length is 100 corresponding to 25 ms, and the lengths of the feedforward filter and feedback filter are 75 ms and 25 ms, respectively. In this mode, the quadrature phase shift keying (QPSK) constellation mapping is utilized.

Before channel estimation and channel equalization, the Doppler is estimated and compensated using match filtering [27]. In the CE-DFE receiver, the channel is estimated via training sequences or symbols after the decision, and the algorithm for channel estimation is the least square. The filter coefficients are obtained by (5) and (6). In order to avoid error propagation, the training symbols are periodically inserted in the transmitted signals, and low-density parity-check (LDPC) coding with a rate of 3/4 is utilized.

Table 2. Parameters setting in mode 2.

Parameter	Notation	Value
Sample frequency (kHz)	f_s	64
Center frequency (kHz)	f_c	15.5
Bandwidth (kHz)	B	4
Modulation system	-	QPSK
Channel length	L	25 ms (100 samples)
Length of feedforward filter	N_{ff}	75 ms (300 samples)
Length of feedback filter	N_{fb}	24.8 ms (99 samples)

Figure 13 shows the results in mode 2. Figure 13a shows the transmitted Sonar picture¹. The transmitted picture is compressed with three colors, where the green part denotes no target, and the blue and yellow colors denote detected targets with different strengths. The SNR of the signals in each hydrophone is 21.5 dB, 29.3 dB, and 25 dB, respectively. Figure 13b shows the picture using the first hydrophone, one may see that, although there is much noise, the outline can be observed. The BER after LDPC decoding in Figure 13b is 0.1721. Looking at Figure 13c, the picture is clearly recovered, and the noise level is extremely low. The BER in Figure 13c is 2.7778×10^{-4} . Since the multiple reception is used, the vertical diversity is used to enhance received SNR. Finally, Figure 13d shows the recovered picture using three hydrophones, one may see that the recovered picture is the same with in Figure 13a, and the BER in Figure 13d is 0.

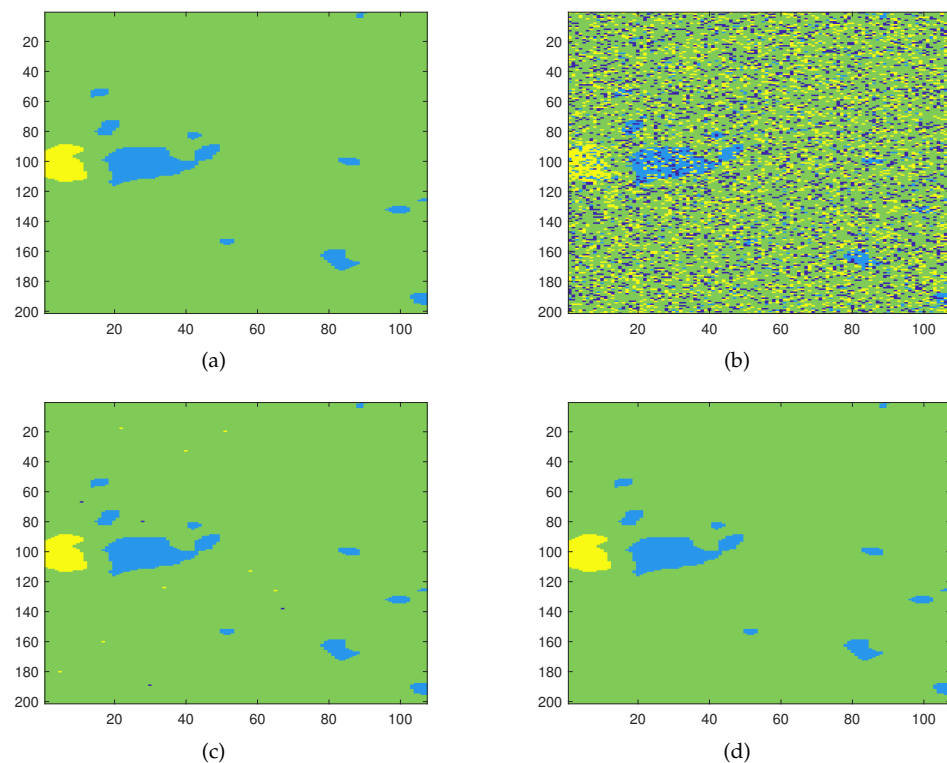


Figure 13. Image transmission results. (a) The transmitted picture. (b) Recovered image through one channel. (c) Recovered image through two channels. (d) Recovered image through three channels.

Mode 2 builds a bridge of signal transmission between the underwater and non-underwater, providing a new solution when some urgent information needs to be recovered in time. Moreover, mode 2 can connect with Cloudy.

3.3. Experimental Results in Mode 3

Since the digital signal processing is performed in the MCU in mode 3, the parameters should be balanced between computational complexity and communication performance. To demonstrate the high reconfigurability, in this mode, the DSSS receiver with different center frequencies is implemented. The parameter setting is shown in Table 3. The sampling frequency was set at 64 kHz, the bandwidth was fixed at 4 kHz, and the length of the gold code is 127. As a result, the length of the DSSS symbol is 32 ms, and the DSSS receiver can handle multi-path that is less than 32 ms. The number of gold codes was set to 128, as a result, the raw data rate is 187.5 bps. The center frequency can be easily adjusted, for example, 9 kHz and 15.5 kHz in this experiment. To avoid the error bits, the convolutional coding technology with a coding rate of 1/2 was used, so the data rate after channel decoding was 93.75 bps.

Table 3. Parameters of DSSS receivers in mode 3.

Parameter	Notation	Value
Sampling frequency (kHz)	f_s	64
Center frequency (kHz)	f_c	9/15.5
Bandwidth (kHz)	B	4
Number of gold code	-	128
Length of gold code	L	127
Symbol length (ms)	T_s	42.7
Code rate of convolutional encoding	-	1/2
Data rate before channel decoding (bps)	R_1	187.5
Data rate after channel decoding (bps)	R_2	93.75

Figure 14 shows the channel estimation results using the signal in mode 3. The signal is obtained from the hydrophone near the surface. It can be seen that the channels exhibit rich multi-path, and the delay is about 80 ms.

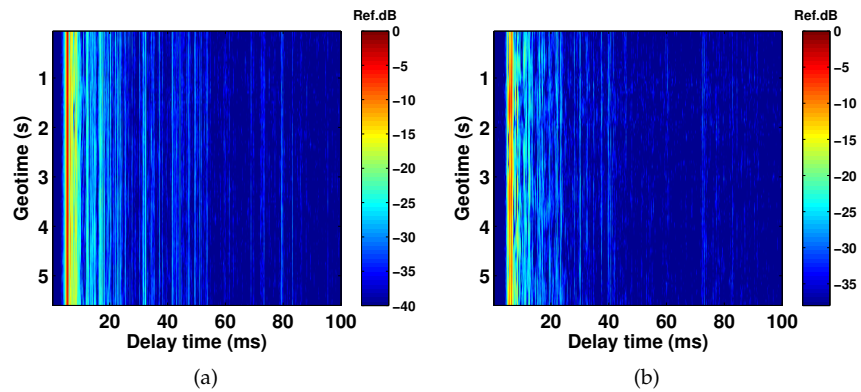


Figure 14. Channel estimation results. (a) Channel estimation result when $f_c = 9$ kHz. (b) Channel estimation result when $f_c = 15.5$ kHz.

Figure 15 shows the corresponding Doppler estimation. From the two subfigures, we can see that the Doppler is insignificant. Since the transmitter and the hydrophones were fixed, the Doppler may be caused by current.

The parameter BER is used to evaluate the communication performance of the DSSS receiver. Figure 16a displays the average BER of the received DSSS signals when $f_c = 15.5$ kHz, the BER is obtained before channel decoding. The BER of seven multi-function hydrophones, numbered sequentially from NO. 1 to NO. 7, are counted, and each multi-function hydrophone contributed 33 frames. It can be found that except for NO. 1 and NO. 2 multi-function hydrophones, the other hydrophones achieved BER, free. Although the first two did not perform perfectly, the BER is still under 10^{-3} , and after convolutional

decoding, the BER is free. Figure 16b shows the BER of the first 19 frames from the first two multi-function hydrophones in detail. It should be noted that the last 14 frames have zero BER. In NO. 1 multi-function hydrophone, only 5 frames exist error bits, while in NO. 2 multi-function hydrophone, the number of frames that exist error bits is 4. It is worth noting that the BER of those nine frames is in the order of 10^{-2} . After channel decoding, the error bits are all corrected, which are error free.

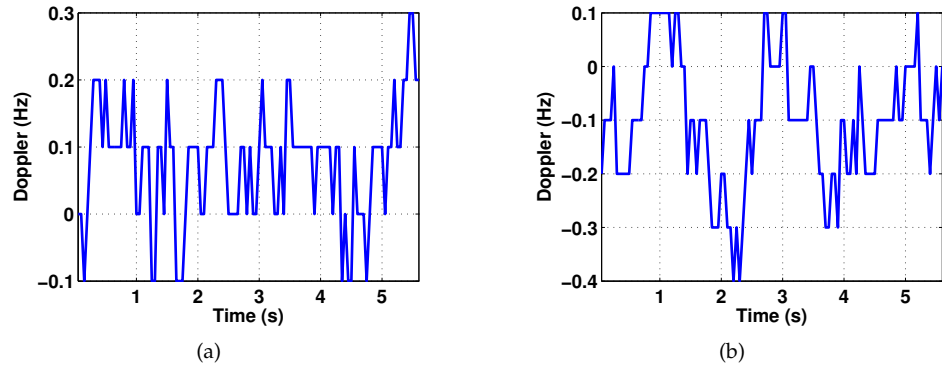


Figure 15. Doppler estimation results. (a) Doppler estimation result when $f_c = 9$ kHz. (b) Doppler estimation result when $f_c = 15.5$ kHz.

The BER obtained from the DSSS receiver whose center frequency is $f_c = 9$ kHz is 0 before and after channel decoding. The reason may be that the low-frequency acoustic signal has lower attenuation, which results in higher SNR.

In conclusion, from the experiments, our proposed multi-function hydrophone has good acquisition and communication quality.

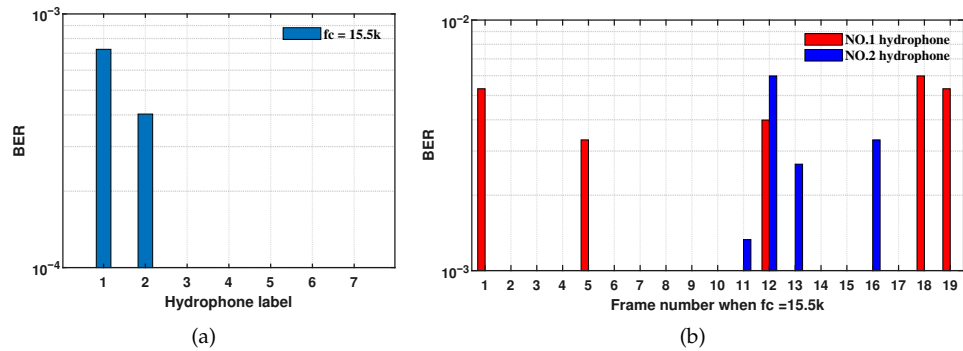


Figure 16. BER when $f_c = 15.5$ kHz. (a) Average BER of each hydrophone. (b) BER of every frame before decoding.

4. Conclusions

Since the increasing development and exploration of the ocean, underwater acoustic transmission and reception have been paid significant attention. In this paper, a multi-function hydrophone for underwater acoustic application was proposed and designed in terms of hardware and software. Particularly, in the hardware part, we added a pre-amplifier with gain control and a high-performance ADC chip, and the MCU was introduced. Moreover, the connection and control among different components were demonstrated. In the software part, the functions of different threads were introduced. Finally, three experiments were conducted to verify the proposed multi-function hydrophone. High-quality underwater signal reception and storage were verified using mode (1). Clear picture recovery was achieved by mode (2). Extremely low BER was obtained via mode (3). The proposed multi-function hydrophone gives a new solution to receive and process the underwater acoustic signals, having potential to build an air-land-ocean Internet of Things network.

Author Contributions: Conceptualization, formal analysis, and writing—review and editing, Y.Z. and R.W.; investigation and writing—original draft preparation, Y.Z. and R.W.; investigation and data curation, X.Y., F.T. and J.W.; Project administration, F.T. All authors have read and agreed to the published version of the manuscript.

Funding: This research was funded by the fundamental Research Funds for the Central Universities (No. 20720210078), and in part by Marine Industry Funding of Xiamen city (No. 22CZB012HJ13).

Institutional Review Board Statement: Not applicable.

Informed Consent Statement: Not applicable.

Data Availability Statement: Data available on request from the corresponding author.

Conflicts of Interest: The authors declare no conflict of interest.

Abbreviations

The following abbreviations are used in this manuscript:

ADC	Analog-to-Digital Converter
ASK	Amplitude Shift Keying
AUV	Autonomous Underwater Vehicle
BER	Bit Error Rate
CE-DFE	Channel Estimation based Decision Feedback Equalizer
CPU	Central Processing Unit
DA-DFE	Direct Adaptive Decision Feedback Equalizer
DMIPS	Dhrystone Million Instructions Per Second
DSP	Digital Signal Processor
DSSS	Direct Sequence Spread Spectrum
DMA	Direct Memory Access
FPU	Floating Point Unit
FTP	File Transfer Protocol
GPIO	General Purpose Input Output
GUI	Graphical User Interface
kSPS	Kilo-Symbols Per Second
LDPC	Low-density Parity-check
LFM	Linear Frequency Modulation
MCASP	Multichannel Audio Serial Port
MCU	Micro-controller Unit
OFDM	Orthogonal Frequency Division Multiplexing
OOK	On-off Keying
OSDM	Orthogonal Signal Division Multiplexing
PN	Pseudo Noise
QPSK	Quadrature Phase Shift Keying
RTC	Real-time Clock
SD	Secure Digital
SNR	Signal to Noise Ratio
SPI	Serial Peripheral Interface
SSP	Sound Speed Profile
ST	STMicroelectronics
TCP/IP	Transmission Control Protocol/Internet Protocol
UDP	User Datagram Protocol
USART	Universal Synchronous/Asynchronous Receiver/Transmitter
UUV	Unmanned Underwater Vehicle
WAV	Waveform

Notes

¹ This picture is from Acoustic and Navigation Laboratory (ANL) in Haifa University, Israel.

References

1. Toma, D.M.; Masmitja, I.; del Río, J.; Martínez, E.; Artero-Delgado, C.; Casale, A.; Figoli, A.; Pinzani, D.; Cervantes, P.; Ruiz, P.; et al. Smart embedded passive acoustic devices for real-time hydroacoustic surveys. *Measurement* **2018**, *125*, 592–605. [CrossRef]
2. Miksis-Olds, J.L.; Nichols, S.M. Is low frequency ocean sound increasing globally? *J. Acoust. Soc. Am.* **2016**, *139*, 501–511. [CrossRef] [PubMed]
3. Kolar, H.R.; McKeown, E.P.; Purcell, M.E.; Gaughan, P.J.; Westbrook, A.G.; Barry, M.G.; Akhriev, A.M.; Hayes, J.P.; Castelfranco, A.; Nolan, G.; et al. The design and deployment of a real-time wide spectrum acoustic monitoring system for the ocean energy industry. In Proceedings of the 2013 MTS/IEEE OCEANS-Bergen, Bergen, Norway, 10–14 June 2013.
4. Hayes, J.P.; Kolar, H.R.; Akhriev, A.; Barry, M.G.; Purcell, M.E.; McKeown, E.P. A real-time stream storage and analysis platform for underwater acoustic monitoring. *IBM J. Res. Dev.* **2013**, *57*, 15:1–15:10. [CrossRef]
5. Liu, L.; Xiao, L.; Lan, S.; Liu, T.-T.; Song, G. Using petrel II glider to analyze underwater noise spectrogram in the south China sea. *Acoust. Aust.* **2018**, *46*, 151–158. [CrossRef]
6. Dassatti, A.; van der Schaar, M.; Guerrini, P.; Zaugg, S.; Houégnigan, L.; Maguer, A.; André, M. On-board underwater glider real-time acoustic environment sensing. In Proceedings of the OCEANS 2011 IEEE—Spain, Santander, Spain, 6–9 June 2011.
7. Chen, T.; Chan, J.; Gollakota, S. Underwater acoustic ranging between smartphones. *arXiv* **2022**, arXiv:2209.01780.
8. Jeon, J.-H.; Hwangbo, S.-H.; Peyvandi, H.; Park, S.-J. Design and implementation of a bidirectional acoustic micro-modem for underwater communication systems. In Proceedings of the 2012 Oceans, Hampton Roads, VA, USA, 14–19 October 2012.
9. Younce, J.; Singer, A.; Riedl, T.; Landry, B.; Bean, A.; Arikan, T. Experimental results with HF underwater acoustic modem for high bandwidth applications. In Proceedings of the 2015 49th Asilomar Conference on Signals, Systems and Computers, Pacific Grove, CA, USA, 8–11 November 2015.
10. Martins, M.S.; Cabral, J.; Lopes, G.; Ribeiro, F. Underwater acoustic modem with streaming video capabilities. In Proceedings of the OCEANS 2015-Genova, Genova, Italy, 18–21 May 2015.
11. Zhou, Y.; Tong, F. Research and development of a highly reconfigurable OFDM MODEM for shallow water acoustic communication. *IEEE Access* **2019**, *7*, 123569–123582. [CrossRef]
12. Yang, X.; Zhou, Y.; Wang, R.; Tong, F. Research and implementation on a real-time OSDM MODEM for underwater acoustic communications. *IEEE Sens. J.* **2023**, *23*, 18434–18448. [CrossRef]
13. Green, D.; McManus, S. Smart modems—Underwater capabilities beyond communications. In Proceedings of the 2012 Oceans-Yeosu, Yeosu, Korea, 21–24 May 2012.
14. Caldas-Morgan, M.; Alvarez-Rosario, A.; Rodrigues Padovese, L. An autonomous underwater recorder based on a single board computer. *PLoS ONE* **2015**, *10*, e0130297. [CrossRef] [PubMed]
15. Ocean Sonics Introduction of Iclisten sc2, Canada. Available online: <https://oceansonics.com/product-types/iclisten-smart-hydrophones/> (accessed on 21 October 2023).
16. Loggerhead Instruments. Snap Recorder, Florida, USA. Available online: <https://www.loggerhead.com/snap> (accessed on 21 October 2023).
17. Cetacean Research Technology. Remote Underwater Digital Acoustic Recorders, USA. Available online: <https://www.cetaceanresearch.com/hydrophone-systems/rudar/index.html> (accessed on 21 October 2023).
18. Ocean Instruments. Soundtrap, New Zealand. Available online: <http://www.oceaninstruments.co.nz/shop/> (accessed on 21 October 2023).
19. Abyssens. Full Technical Specifications of DORI Recorders, Brittany, France. Available online: <https://www.abysens.fr/underwater-acoustic-recorders-dori/> (accessed on 21 October 2023).
20. Analog Devices, Inc. *AD620: Low Cost Low Power Instrumentation Amplifier*; Rev, H., Ed.; Analog Devices, Inc.: Norwood, MA, USA, 2009.
21. Analog Devices, Inc. *LTC6910: Digitally Controlled Programmable Gain Amplifiers in SOT-23 Data Sheet*; Rev, B., Ed.; Analog Devices, Inc.: Norwood, MA, USA, 2017.
22. STMicroelectronics Product Overview of STM32H743XI. Available online: <https://www.st.com/en/microcontrollers-microprocessors/stm32h743xi.html> (accessed on 21 October 2023).
23. Poisel, R.A. *Modern Communications Jamming Principles and Techniques*, 2nd ed.; Artech House, Inc.: Norwood, MA, USA, 2011.
24. Kochanska, I.; Salamon, R.; Schmidt, J.; Schmidt, A. Study of the Performance of DSSS UAC System Depending on the System Bandwidth and the Spreading Sequence. *Sensors* **2021**, *21*, 2484–2504. [CrossRef] [PubMed]
25. Zhou, Y.; Tong, F.; Song, A.; Diamant, R. Exploiting spatial-temporal joint sparsity for underwater acoustic multiple-input-multiple-output communications. *IEEE J. Ocean. Eng.* **2020**, *46*, 142–149. [CrossRef]
26. Preisig, J. Performance analysis of adaptive equalization for coherent acoustic communications in the time-varying ocean environment. *J. Acoust. Soc. Am.* **2005**, *118*, 264–278. [CrossRef] [PubMed]
27. Zhou, Y.; Song, A.; Tong, F.; Kastner, R. Distributed compressed sensing based channel estimation for underwater acoustic multiband transmissions. *J. Acoust. Soc. Am.* **2018**, *143*, 3985–3996. [CrossRef] [PubMed]

Disclaimer/Publisher’s Note: The statements, opinions and data contained in all publications are solely those of the individual author(s) and contributor(s) and not of MDPI and/or the editor(s). MDPI and/or the editor(s) disclaim responsibility for any injury to people or property resulting from any ideas, methods, instructions or products referred to in the content.